



Supplementary Materials for

Susceptibility of ferrets, cats, dogs, and other domesticated animals to SARS–coronavirus 2

Jianzhong Shi*, Zhiyuan Wen*, Gongxun Zhong*, Huanliang Yang*, Chong Wang*, Baoying Huang*, Renqiang Liu, Xijun He, Lei Shuai, Ziruo Sun, Yubo Zhao, Peipei Liu, Libin Liang, Pengfei Cui, Jinliang Wang, Xianfeng Zhang, Yuntao Guan, Wenjie Tan, Guizhen Wu†, Hualan Chen†, Zhigao Bu†

*These authors contributed equally to this work.

†Corresponding author. Email: buzhighao@caas.cn (Z.B.); chenhualan@caas.cn (H.C.); wugz@ivdc.chinacdc.cn (G.W.)

Published 8 April 2020 on *Science* First Release

DOI: 10.1126/science.abb7015

This PDF file includes:

Materials and Methods
Supplementary Text
Figs. S1 to S10
Table S1
References

Other Supplementary Material for this manuscript includes the following:

(available at science.sciencemag.org/cgi/content/full/science.abb7015/DC1)

MDAR Reproducibility Checklist (.pdf)

Materials and Methods

Facility, Ethics, and Biosafety statement

All experiments with infectious SARS-CoV-2 were performed in the biosafety level 4 and animal biosafety level 4 facilities in the Harbin Veterinary Research Institute (HVRI) of the Chinese Academy of Agricultural Sciences (CAAS), which is approved for such use by the Ministry of Agriculture and Rural Affairs of China. The animal studies were carried out in strict accordance with the recommendations in the Guide for the Care and Use of Laboratory Animals of the Ministry of Science and Technology of the People's Republic of China. The protocols were approved by the Committee on the Ethics of Animal Experiments of the HVRI of CAAS (Approval number 2020-01-01JiPi).

All experiments were conducted within the biosafety level 4 (P4) facilities in the Harbin Veterinary Research Institute (HVRI) of the Chinese Academy of Agricultural Sciences (CAAS), which was completed in 2015 and accredited by the China National Accreditation Service for Conformity Assessment in 2018. Handling of SARS-CoV-2 was approved by the Ministry of Agriculture and Rural Affairs of China on January 22, 2020 and by the National Health Commission of China on January 31, 2020. All activities inside the P4 labs are monitored by trained guards via video cameras. Only authorized personnel that have received appropriate training can access the P4 facility. Experienced personnel work in pairs in the facilities. Our staff wear powered air-purifying respirators that filter the air, and disposable coveralls (fig. S10A) when they culture the virus and handle animals (ferrets and cats) that are in isolators, and wear full body, air-supplied, positive pressure suits (fig. S10B) when they perform studies involving the use of dogs, pigs, chickens, and ducks, which are kept in a room (not in isolators); the researchers are disinfected before they leave the room and then shower on exiting the facility. The facility is secured by appropriate procedures approved by the HVRI institutional biosafety officers. All facilities, procedures, training records, safety drills, and inventory records are subject to periodic inspections and ongoing oversight by the institutional biosafety officers who consult frequently with the facility managers. The research program, procedures, occupational health plan, security, and facilities are reviewed annually by a Ministry of Agriculture and Rural Affairs official

Cells

Vero-E6 cells were obtained from ATCC (ATCC CRL-1586) and maintained in Dulbecco's modified Eagle's medium (DMEM) containing 10% fetal bovine serum (FBS) and antibiotics and incubated at 37°C with 5% CO₂.

Virus

SARS-CoV-2 strain BetaCoV/Wuhan/IVDC-HB-01/2019 (C-Tan-HB01) (GISAID accession no. EPI_ISL_402119) [formally designated as SARS-CoV-2/CTan/human/2019/Wuhan (CTan-H) in this study] was isolated from a human patient (2) and SARS-CoV-2 strain BetaCoV/Wuhan/IVDC-HB-envF13-20/2020 (F13) (GISAID accession no. EPI_ISL_408514) [formally designated as SARS-CoV-2/F13/environment/2020/Wuhan(F13-E) in this study] was isolated from an environmental sample collected in Huanan seafood market, Wuhan. The two viruses differ in two nucleotides in their non-coding region: CTan-H bears 15C and 48C, whereas

F13-E bears 15T and 48A. Viral stocks were prepared in Vero E6 cells with DMEM containing 2% FBS, 5 ug/ml TPCK-trypsin, and 30 mmol/L MgCl₂. Viruses were harvested and the titers were determined by means of plaque assay in Vero E6 cells.

qPCR

To quantitate the viral RNA copies in the samples collected from the animals, viral RNA was extracted by using a QIAamp vRNA Minikit (Qiagen, Hilden, Germany). Reverse transcription was performed by using the HiScript® II Q RT SuperMix for qPCR (Vazyme, Nanjing, China). qPCR was conducted by using the Applied Biosystems® QuantStudio® 5 Real-Time PCR System (Thermo Fisher Scientific, Waltham, MA, USA) with Premix Ex Taq™ (Probe qPCR), Bulk (TaRaKa, Dalian, China). The N gene-specific primers (forward, 5'-GGGGAAGCTTCTCCTGCTAGAAT-3'; reverse, 5'-CAGACATTTTGCTCTCAAGCTG-3') and probe (5'-FAM-TTGCTGCTGCTTGACAGATT-TAMRA-3') were utilized according to the information provided by the National Institute for Viral Disease Control and Prevention, China (<http://nmdc.cn/nCoV>). The amount of vRNA for the target SARS-CoV-2 N gene was normalized to the standard curve obtained by using a plasmid (pBluescriptIISK-N, 4,221 bp) containing the full-length cDNA of the SARS-CoV-2 N gene.

ELISA

Antibodies against SARS-CoV-2 were detected by using a Double Antigen Sandwich ELISA Kit (ProfTech, Luoyang, China) according to the manufacturer's instructions. Briefly, 100 µL of sera were added to an antigen-precoated microtiter plate and incubated at 37 °C for 30 min. Plates were then washed 5 times with PBST, and incubated with HRP-conjugated antigen at 37 °C for 30 min. Plates were washed 5 times with PBST, and 100 µL of substrate solution was added to enable colorimetric analysis. The reaction was stopped by adding 50 µL of stop buffer, and optical density (OD) was measured at 450 nm. OD₄₅₀ value greater than 0.2 is considered positive for seroconversion according to the manufacturer's instructions.

Animal studies

Randomization and blinding were not used for the allocation of animals to experimental groups. The number of animals used in each study was similar as reported in previous publications (20, 22, 33, 34) or was determined by following the “minimum-quantity-principle” in our protocol. All of the animal studies were performed for one time, and the biological replicates (number of animals used in each experiment) were indicated in detail below.

Ferret Study

Three- to four-month-old female ferrets (Wuxi Cay Ferret Farm, Wuxi, China) were used in this study. Groups of five ferrets were anesthetized with Zoletil 50 (Virbac, Carros, France) and inoculated intranasally with 10⁵ plaque forming unit (PFU) of SARS-CoV-2 CTan-H or F13-E in a volume of 1 mL and each ferret was housed in a separate cage inside an isolator (20, 22, 33, 34). Two ferrets from each group were euthanized on day 4 post-inoculation (p.i.) and their organs and tissues, including lungs, tracheas, nasal turbinates, soft palates, brains, hearts, tonsils, kidneys, spleens, livers, pancreas, and

small intestines, were collected for viral RNA and virus detection. Nasal washes and rectal swabs were collected from the other three ferrets on days 2, 4, 6, 8, and 10 p.i. for viral RNA and virus detection. Body weights and body temperature were monitored every other day. The ferrets were scheduled to be euthanized on day 20 p.i. to assess them for antibodies against SARS-CoV-2 by using the Double Antigen Sandwich ELISA kit (ProfTech, Luoyang, China) and by use of a neutralization assay.

Eight ferrets were also inoculated intratracheally with 10^5 PFU of CTan-H. On days 2, 4, 8, and 14 p.i., two ferrets were each euthanized, and their organs were collected for virus detection.

Cat study

Male/female mixed ten outbred domestic juvenile cats (aged 70–100 days) and ten outbred subadult cats (aged 6–9 months), obtained from the National Engineering Research Center of Veterinary Biologics CORP. (Harbin, China) were used in this study. To evaluate the replication of SARS-CoV-2, four juvenile cats and four subadult cats were intranasally inoculated with 10^5 PFU of CTan-H. Two cats of each age group were euthanized on day 3 p.i. and day 6 p.i., respectively. Organs and tissues were collected for viral RNA detection, virus titration in Vero E6 cells, and histological studies.

To investigate the transmissibility of SARS-CoV-2 in cats, six cats (three subadult and three juvenile) were anesthetized with Zoletil 50 and inoculated intranasally with 10^5 PFU of CTan-H. Each animal was housed in a specially designed cage inside an isolator (20, 22, 33, 34), the schematic presentation of the isolator and cages are shown in Figure S10. Twenty-four hours later, a similar-aged naive cat was placed in an adjacent cage (4 cm away), separated by a double-layered net divider (fig. S10C). The ambient conditions were set at 20–22°C and 30%–40% relative humidity. The airflow in the isolator was horizontal with a speed of 0.1 m/s; the airflow direction was from the inoculated animals to the exposed animals. Feces were collected on days 3, 5, 7, and 9 p.i. from the subadult cats, and nasal washes were collected from the juvenile cats on days 2, 4, 6, 8 and 10 p.i. for viral RNA detection. One pair and two pairs of the subadult cats were euthanized on days 11 and 12 p.i., respectively, and their organs, including lungs, tracheas, nasal turbinates, soft palates, tonsils, brains, hearts, submaxillary lymph nodes, kidneys, spleens, livers, pancreas, and small intestines, were collected for viral RNA detection. Animals were anesthetized during the process of the nasal wash or blood collection, and exposed animals were always handled first. Sera were collected from subadult cats on the days they were euthanized, and sera were collected from the juvenile cats on days 10 and 20 p.i. Antibodies against SARS-CoV-2 were detected by using the Double Antigen Sandwich ELISA kit (ProtTech, Luoyang, China) and a neutralization assay.

Dog, pig, chicken, and duck study

To assess the susceptibility of dogs, pigs, chickens, and ducks to SARS-CoV-2, three-month-old beagles (Kangping Institute, Shenyang, China), male/female mixed 40-day-old specific-pathogen-free (SPF) Landrace and Large White pigs (HVRI, Harbin, China), 4-week-old specific-pathogen-free (SPF) White Leghorn chickens (HVRI, Harbin, China), and 4-week-old SPF ducks (Shaoxin ducks, a local bred) (HVRI, Harbin, China) were used in this study.

Five animals of each species were intranasally inoculated with 10^5 PFU (dogs and pigs) or $10^{4.5}$ PFU (chickens and ducks) of CTan-H, and two (dogs) or three (pigs, chickens, ducks) uninfected animals were housed in the same room with their infected counterparts to monitor the transmission of CTan-H. Oropharyngeal and rectal swabs from all animals were collected every other day for viral RNA detection. One beagle was viral RNA positive by its rectal swab on day 2 p.i. and was euthanized on day 4 p.i.; its organs, including nasal turbinates, soft palates, tonsils, tracheas, lungs, brains, hearts, kidneys, spleens, livers, pancreas, and small intestines, were collected for viral RNA detection by qPCR. Sera were collected from all remaining animals on day 14 p.i., and antibodies against SARS-CoV-2 were detected by using a Double Antigen Sandwich ELISA kit (ProtTech, Luoyang, China).

Plaque reduction neutralization test

SARS-CoV-2 CTan-H strain (100 PFU) was incubated with two-fold serial dilutions of sera for 1 h at 37°C. A plaque assay was then performed in Vero E6 cells with the neutralization mixtures. Neutralizing antibody titers were calculated as the maximum serum dilution yielding a 50% reduction in the number of plaques relative to control serum prepared from uninfected animals.

Histological study

Tissues of animals were fixed in 10% neutral-buffered formalin, embedded in paraffin, and cut into 4- μ m sections. The sections were stained with hematoxylin-eosin (H&E) or used in immunohistochemical (IHC) assays. The sections used for immunohistochemistry were dewaxed in xylene and hydrated through a series of descending concentrations of alcohol to water. For viral antigen retrieval, sections were immersed in citric acid/sodium citrate solution at 121 °C for 15 minutes. After cooling, the sections were treated with 3% hydrogen peroxide for 30 minutes to remove endogenous peroxidase activity and blocked with 8% skim milk to reduce nonspecific binding. After three 5-minute washes in TBS, the sections were incubated with rabbit anti-SARS-CoV-2 nucleoprotein monoclonal antibody (1:500; Frdbio. Wuhan, China; catalog number: nCov-N-rmAb) in 8% skim milk at 4 °C overnight. The sections were then washed again with TBS and incubated with anti-rabbit IgG (whole molecule)-HRP (1:600, Sigma-Aldrich, catalog number: A-9169) at room temperature for 60 minutes. The immunostaining was visualized with DAB and counterstained with hematoxylin.

Virus attachment study

Attachment of SARS-CoV-2 virus to lung tissues of ferrets were tested as described previously with H5N1 influenza virus (35), with slight modification. Neutral buffered formalin-fixed health ferret lungs were processed into paraffin-embedded tissue sections. After dewaxing with xylene and hydrating with alcohol, β -propiolactone inactivated SARS-CoV-2 at a concentration of 5×10^7 PFU/ml was added to sections and incubated at 4 °C overnight. After extensive washing in triethanolamine-buffered saline (TBS) buffer, sections were incubated with mouse serum anti recombinant SARS-CoV-2 S protein and then HRP-conjugated goat anti-mouse IgG (H+L) secondary antibody (1:400, Invitrogen, catalog number: 31430) at room temperature for 1 hour. The immunostaining was

visualized with diaminobenzidine (DAB) and counterstained with hematoxylin. Omission of incubation with inactivated virus was used as a negative control.

Supplementary Text

Histopathologic and immunohistochemical studies

Histopathologic and immunohistochemical studies were performed on samples from the virus-inoculated juvenile cats that died or euthanized on day 3 p.i. The nasal respiratory mucosa epithelium exhibited an abnormal arrangement with loss of cilia accompanied by lymphocyte infiltration into the lamina propria (fig. S7A). In the tonsils, the surface of the epithelium was covered with abundant neutrophils and cellular debris, and the epithelial cells showed varying degrees of degeneration and necrosis (fig. S7B). The tracheal mucosa was covered with cellular debris and mucous material, altered polarity, degeneration, and necrosis was observed in the epithelial cells (fig. S7C), and epithelial necrosis and lymphocyte infiltration were observed in the submucosal glands (fig. S7D). Inflammatory cell (including neutrophils, mononuclear cells, lymphocytes) aggregation and fibrin formation in the lung vasculature were seen (fig. S7F), infiltration of a large number of macrophages and lymphocytes into the alveolar spaces and interalveolar septa (fig. S7G), and intra-alveolar edema and congestion in the interalveolar septa were commonly observed (fig. S7H). In the small intestine, diffuse degeneration of mucosal epithelial cells was observed, some of which showed necrosis, and moderate lymphocytic infiltration was observed in the mucosal lamina propria (fig. S7I). Large amounts of viral antigen were detected in the epithelium of the nasal respiratory mucosa (fig. S7J) and in the epithelial cells of the tonsils; tonsillar surficial cellular debris was evident (fig. S7K). Although viral antigen was hardly detected in the tracheal epithelial cells, it was highly apparent in the serous cells of the tracheo-bronchial submucosal glands (fig. S7L). Numerous epithelial cells of the small intestine also showed strong positive staining for viral antigen (fig. S7M).

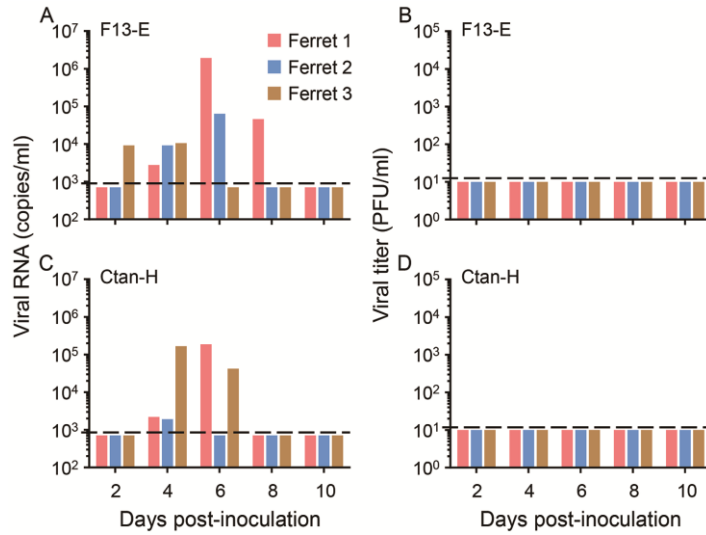


Fig. S1. Replication of SARS-CoV-2 in digestive tract of ferrets.

Viral RNA in rectal swabs of ferrets inoculated with F13-E (A) and CTan-H (C). Viral titer in rectal swabs of ferrets inoculated with F13-E (B) and CTan-H (D). Each color bar represents the value from an individual animal. The horizontal dashed lines indicate the lower limit of detection.

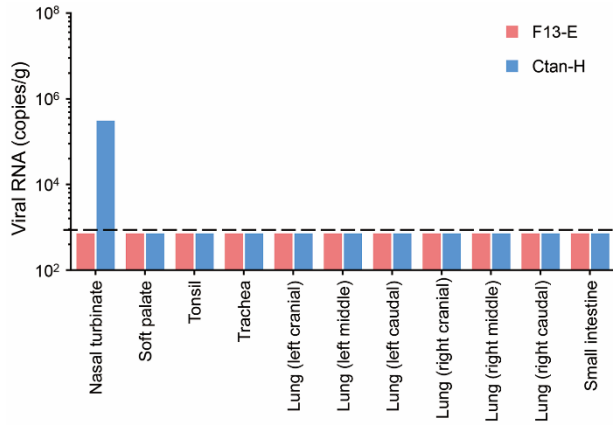


Fig. S2. Replication of SARS-CoV-2 in ferrets.

Ferrets inoculated with F13-E virus or CTan-H virus were euthanized on day 13 p.i. and their organs and tissues were collected for viral RNA detection. Each color bar represents the value from an individual animal. The horizontal dashed lines indicate the lower limit of detection.

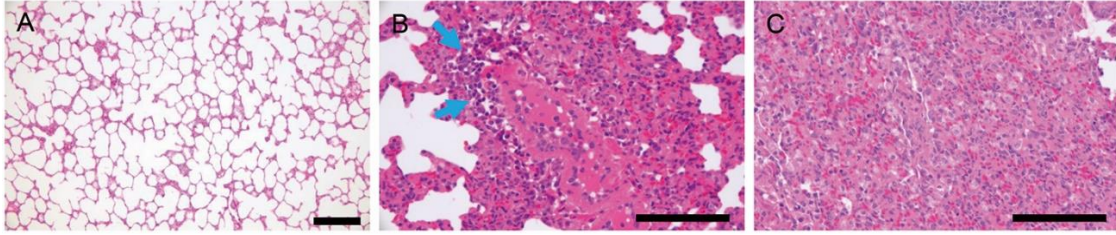


Fig. S3. Histological study of a lung sample from a ferret infected with SARS-CoV-2 CTan-H.

(A) Lung from uninfected animal shows normal structure. (B) Severe lymphoplasmacytic perivascularitis and vasculitis (arrow). (C) Increased numbers of Type II pneumocytes, macrophages, and neutrophils in the alveolar septa and alveolar lumen. Scale bar in A = 200 μm , in B, C = 100 μm .

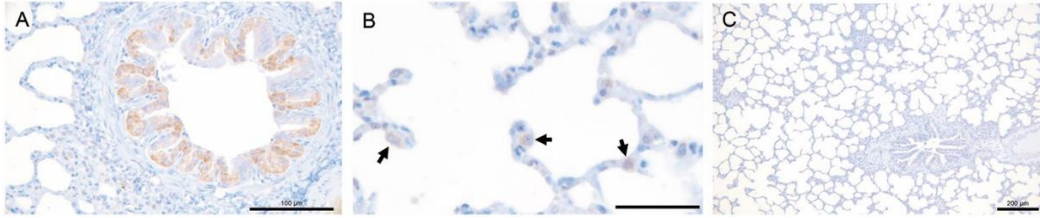


Fig. S4. Attachment of SARS-CoV-2 to lung of ferrets.

(A) Attachment of SARS-CoV-2 to a bronchiole as indicated as brown positive signals in epithelial cells. (B) Attachment of SARS-CoV-2 to type II pneumocytes (arrows). (C) No positive signal observed in negative control without incubation of inactivated SARS-CoV-2. Scale bar in A = 100 μm , in B = 50 μm , in C = 200 μm .

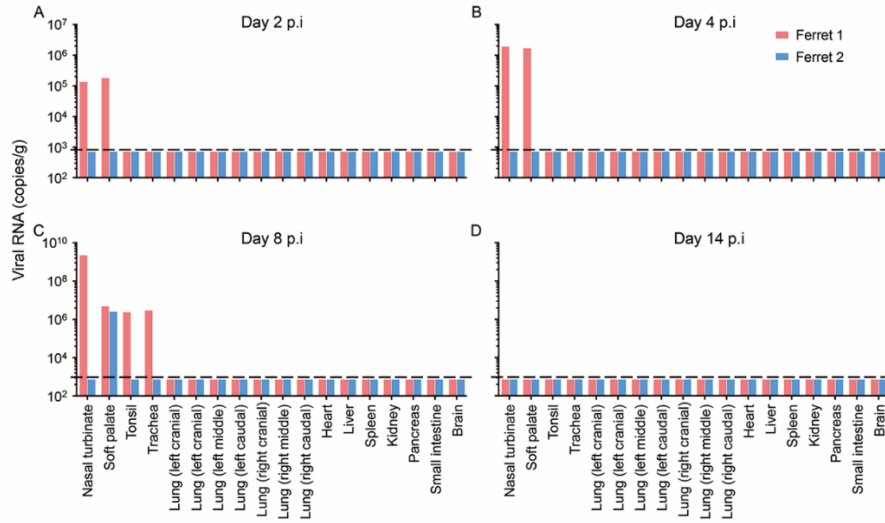


Fig. S5. Viral RNA copies in the organs of ferrets intratracheally inoculated with CTan-H.

Eight ferrets were inoculated intratracheally with 10^5 PFU of CTan-H. On days 2, 4, 8, and 14 p.i., two ferrets were each euthanized, and their organs were collected for virus detection by qPCR. Each color bar represents the value from an individual animal. The horizontal dashed lines indicate the lower limit of detection.

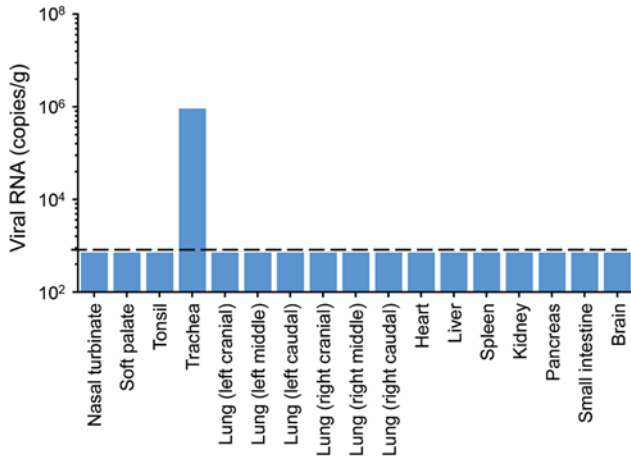


Fig. S6. Viral RNA in organs of a juvenile cat that died on day 13 post inoculation with the CTan-H virus in the transmission study.

The horizontal dashed lines indicate the lower limit of detection.

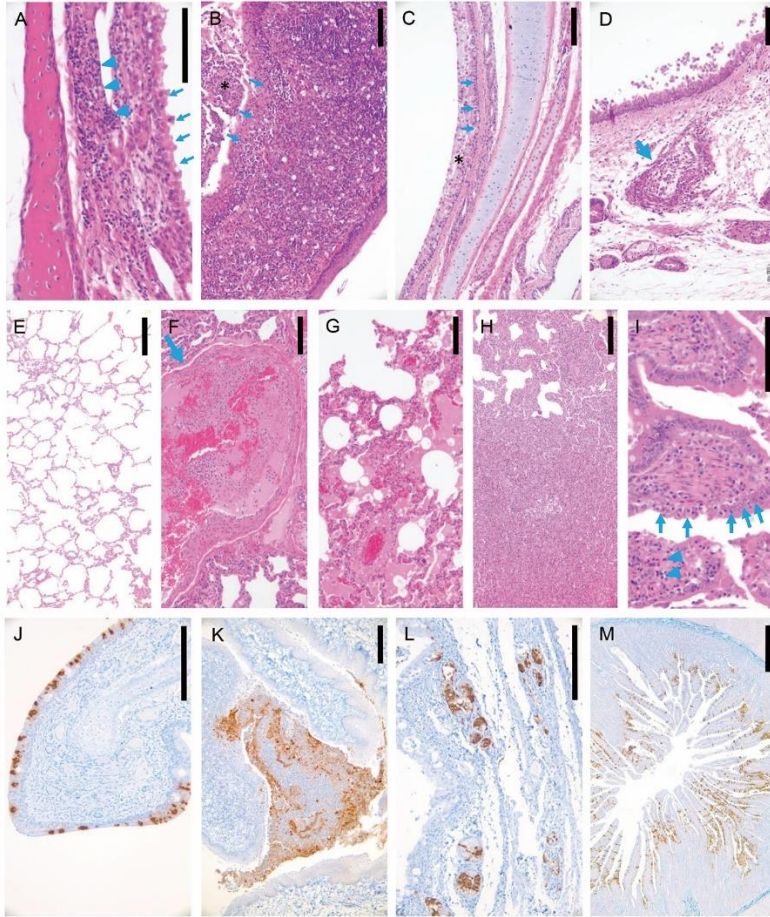


Fig. S7. Histopathologic and immunohistochemical studies.

Histopathologic and immunohistochemical studies were performed on samples from the virus-inoculated juvenile cats that died or euthanized on day 3 p.i. **(A)** Nasal respiratory mucosa, abnormal arrangement of the epithelium with loss of cilia (arrow) and lymphocytic infiltration into the lamina propria (arrow head). **(B)** Tonsil, epithelial degeneration and necrosis with numerous neutrophils (arrow) and cellular debris on the surface of the epithelium (asterisk). **(C)** Trachea, degeneration and necrosis of epithelial cells (arrow) accompanied by coverage with cellular debris and mucous material on the surface of the mucosa (asterisk). **(D)** Tracheae, epithelial necrosis and lymphocyte infiltration in the submucosal glands (arrow). **(E)** Lung from uninfected animal shows normal structure. **(F)** Lung, inflammatory cell aggregation and fibrin formation within a blood vessel (arrow). **(G)** Lung, infiltration of a large number of macrophages and lymphocytes into the alveolar spaces and interalveolar septa. **(H)** Lung, intra-alveolar edema and congestion in the interalveolar septa. **(I)** Small intestine, diffuse degeneration of mucosal epithelial cells, some of which showed necrosis (arrow), and moderate lymphocytic infiltration in the mucosal lamina propria. **(J)** Nasal turbinate, viral antigen in the epithelial cells of the respiratory mucosa. **(K)** Tonsils, viral antigen in the cellular debris and some of the epithelial cells. **(L)** Trachea, viral antigen in the serous cells of the submucosal glands. **(M)** Small intestine, viral antigen in the epithelial cells of the mucosa. Scale bar in A, I = 100 μm , in B-H, J-L = 200 μm , in M = 500 μm .

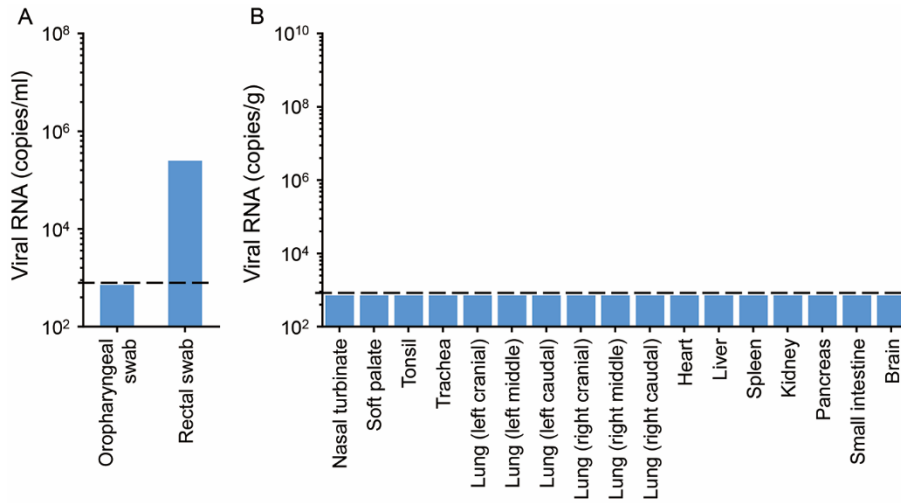


Fig. S8. Viral RNA detection in swabs and organs of a dog infected with CTan-H virus.

(A) Viral RNA in swabs collected on day 2 p.i. (B) Viral RNA in organs or tissues of a dog that was euthanized on day 4 p.i. The horizontal dashed lines indicate the lower limit of detection.

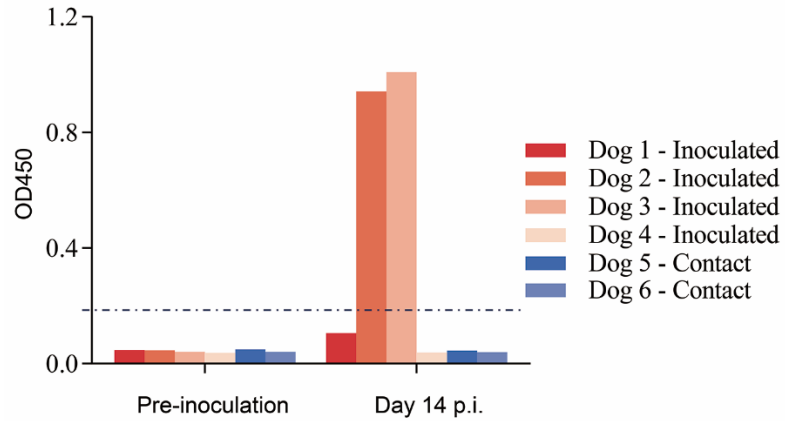


Fig. S9. Seroconversion of CTan-H-inoculated and contact dogs.

Three-month-old beagles were inoculated with 10^5 PFU of CTan-H. Uninfected animals (contact) were housed in the same room with their infected counterparts to monitor the transmission of CTan-H. Sera were collected from animals before inoculation and on day 14 p.i., and antibodies against SARS-CoV-2 were detected by using a Double Antigen Sandwich ELISA kit (ProtTech, Luoyang, China). Optical density (OD450) values greater than 0.2 (horizontal dashed line) were considered positive for seroconversion according to the manufacturer's instructions. Each color bar represents the value from an individual animal.

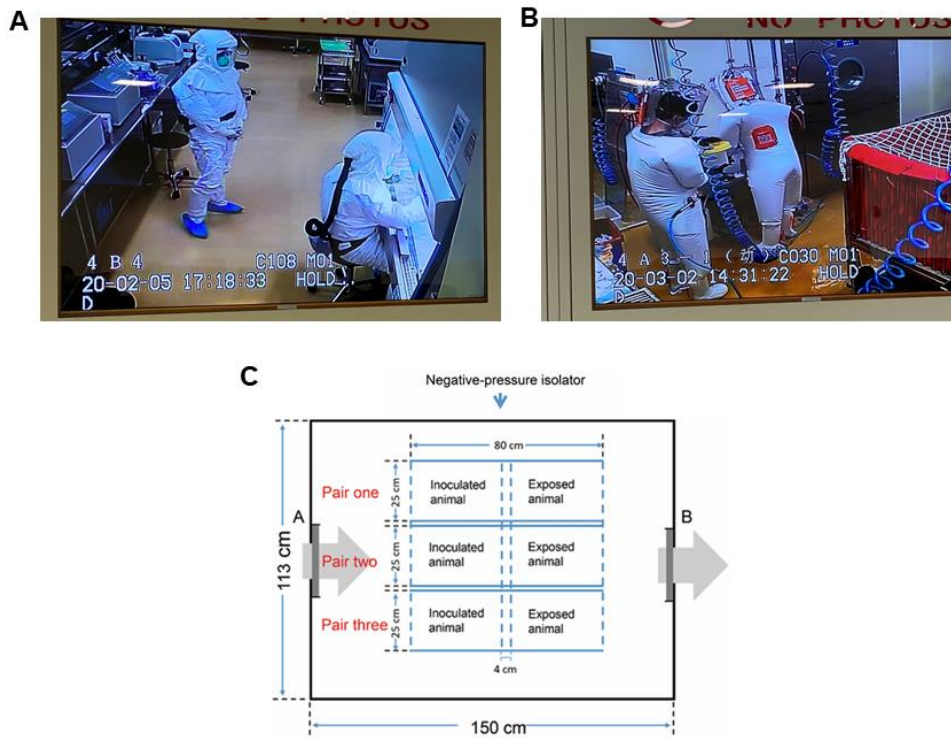


Fig. S10. Images showing personal protective clothing and schematic presentation of the cat transmission study.

(A) Researchers wear powered air-purifying respirators that filter the air, and disposable coveralls when they culture the virus and handle animals (ferrets and cats) that are in isolators. (B) Researchers wear full body, air-supplied, positive pressure suits when they perform studies involving the use of dogs, pigs, chickens, and ducks, which are kept in a room (not in isolators). (C) The transmission cages were specifically designed to allow transmission experiments to be conducted in negatively pressurized isolators (150 cm x 113 cm x 80 cm) in the ABSL4+ facility. The animals were housed in a clear solid steel cage (25 cm x 80 cm x 37 cm), which was divided into 2 small cages (25 cm x 38 cm x 37 cm) by a double-layered net divider (the neighboring cages were 4 cm apart). Twenty-four hours after the three inoculated animals were placed into the cages, three naïve animals were placed in the adjacent cages. Negative pressure within the isolator cage was used to direct a modest (0.1m/sec) flow of HEPA-filtered air (A) from the inoculated to the naïve animals. The outlet airflow (B) was HEPA-filtered to prevent continuous circulation of infectious influenza virus particles.

Table S1. Amino acids at SARS-CoV-2 spike-contacting positions of ACE2 protein.

Origin	Amino acid residues at the SARS-CoV-2 spike-contacting positions of ACE2 protein																			
	24	27	28	30	31	34	35	37	38	41	42	45	82	83	330	353	354	355	357	393
Human	Q	T	F	D	K	H	E	E	D	Y	Q	L	M	Y	N	K	G	D	R	R
Cat	L	.	.	E	E	.	.	.	T
Ferret	L	.	.	E	.	Y	.	.	E	.	.	.	T	.	.	.	R	.	.	.

References and Notes

1. L. Zou, F. Ruan, M. Huang, L. Liang, H. Huang, Z. Hong, J. Yu, M. Kang, Y. Song, J. Xia, Q. Guo, T. Song, J. He, H.-L. Yen, M. Peiris, J. Wu, SARS-CoV-2 Viral Load in Upper Respiratory Specimens of Infected Patients. *N. Engl. J. Med.* **382**, 1177–1179 (2020). [doi:10.1056/NEJMc2001737](https://doi.org/10.1056/NEJMc2001737) [Medline](#)
2. N. Zhu, D. Zhang, W. Wang, X. Li, B. Yang, J. Song, X. Zhao, B. Huang, W. Shi, R. Lu, P. Niu, F. Zhan, X. Ma, D. Wang, W. Xu, G. Wu, G. F. Gao, W. Tan; China Novel Coronavirus Investigating and Research Team, A Novel Coronavirus from Patients with Pneumonia in China, 2019. *N. Engl. J. Med.* **382**, 727–733 (2020). [doi:10.1056/NEJMoa2001017](https://doi.org/10.1056/NEJMoa2001017) [Medline](#)
3. P. Zhou, X.-L. Yang, X.-G. Wang, B. Hu, L. Zhang, W. Zhang, H.-R. Si, Y. Zhu, B. Li, C.-L. Huang, H.-D. Chen, J. Chen, Y. Luo, H. Guo, R.-D. Jiang, M.-Q. Liu, Y. Chen, X.-R. Shen, X. Wang, X.-S. Zheng, K. Zhao, Q.-J. Chen, F. Deng, L.-L. Liu, B. Yan, F.-X. Zhan, Y.-Y. Wang, G.-F. Xiao, Z.-L. Shi, A pneumonia outbreak associated with a new coronavirus of probable bat origin. *Nature* **579**, 270–273 (2020). [doi:10.1038/s41586-020-2012-7](https://doi.org/10.1038/s41586-020-2012-7) [Medline](#)
4. F. Wu, S. Zhao, B. Yu, Y.-M. Chen, W. Wang, Z.-G. Song, Y. Hu, Z.-W. Tao, J.-H. Tian, Y.-Y. Pei, M.-L. Yuan, Y.-L. Zhang, F.-H. Dai, Y. Liu, Q.-M. Wang, J.-J. Zheng, L. Xu, E. C. Holmes, Y.-Z. Zhang, A new coronavirus associated with human respiratory disease in China. *Nature* **579**, 265–269 (2020). [doi:10.1038/s41586-020-2008-3](https://doi.org/10.1038/s41586-020-2008-3) [Medline](#)
5. A. Wu, Y. Peng, B. Huang, X. Ding, X. Wang, P. Niu, J. Meng, Z. Zhu, Z. Zhang, J. Wang, J. Sheng, L. Quan, Z. Xia, W. Tan, G. Cheng, T. Jiang, Genome Composition and Divergence of the Novel Coronavirus (2019-nCoV) Originating in China. *Cell Host Microbe* **27**, 325–328 (2020). [doi:10.1016/j.chom.2020.02.001](https://doi.org/10.1016/j.chom.2020.02.001) [Medline](#)
6. C. Wang, P. W. Horby, F. G. Hayden, G. F. Gao, A novel coronavirus outbreak of global health concern. *Lancet* **395**, 470–473 (2020). [doi:10.1016/S0140-6736\(20\)30185-9](https://doi.org/10.1016/S0140-6736(20)30185-9) [Medline](#)
7. Y. Pan, D. Zhang, P. Yang, L. L. M. Poon, Q. Wang, Viral load of SARS-CoV-2 in clinical samples. *Lancet Infect. Dis.* **20**, 411–412 (2020). [doi:10.1016/S1473-3099\(20\)30113-4](https://doi.org/10.1016/S1473-3099(20)30113-4) [Medline](#)
8. X. Pan, D. Chen, Y. Xia, X. Wu, T. Li, X. Ou, L. Zhou, J. Liu, Asymptomatic cases in a family cluster with SARS-CoV-2 infection. *Lancet Infect. Dis.* **20**, 410–411 (2020). [doi:10.1016/S1473-3099\(20\)30114-6](https://doi.org/10.1016/S1473-3099(20)30114-6) [Medline](#)
9. R. Lu, X. Zhao, J. Li, P. Niu, B. Yang, H. Wu, W. Wang, H. Song, B. Huang, N. Zhu, Y. Bi, X. Ma, F. Zhan, L. Wang, T. Hu, H. Zhou, Z. Hu, W. Zhou, L. Zhao, J. Chen, Y. Meng, J. Wang, Y. Lin, J. Yuan, Z. Xie, J. Ma, W. J. Liu, D. Wang, W. Xu, E. C. Holmes, G. F. Gao, G. Wu, W. Chen, W. Shi, W. Tan, Genomic characterisation and epidemiology of 2019 novel coronavirus: Implications for virus origins and receptor binding. *Lancet* **395**, 565–574 (2020). [doi:10.1016/S0140-6736\(20\)30251-8](https://doi.org/10.1016/S0140-6736(20)30251-8) [Medline](#)
10. P. Liu, X. Z. Tan, 2019 Novel Coronavirus (2019-nCoV) Pneumonia. *Radiology* **295**, 19 (2020). [doi:10.1148/radiol.2020200257](https://doi.org/10.1148/radiol.2020200257) [Medline](#)
11. Q. Li, X. Guan, P. Wu, X. Wang, L. Zhou, Y. Tong, R. Ren, K. S. M. Leung, E. H. Y. Lau, J. Y. Wong, X. Xing, N. Xiang, Y. Wu, C. Li, Q. Chen, D. Li, T. Liu, J. Zhao, M. Liu, W. Tu, C. Chen, L. Jin, R. Yang, Q. Wang, S. Zhou, R. Wang, H. Liu, Y.

- Luo, Y. Liu, G. Shao, H. Li, Z. Tao, Y. Yang, Z. Deng, B. Liu, Z. Ma, Y. Zhang, G. Shi, T. T. Y. Lam, J. T. Wu, G. F. Gao, B. J. Cowling, B. Yang, G. M. Leung, Z. Feng, Early Transmission Dynamics in Wuhan, China, of Novel Coronavirus-Infected Pneumonia. *N. Engl. J. Med.* **382**, 1199–1207 (2020). [doi:10.1056/NEJMoa2001316](https://doi.org/10.1056/NEJMoa2001316) [Medline](#)
12. C. Huang, Y. Wang, X. Li, L. Ren, J. Zhao, Y. Hu, L. Zhang, G. Fan, J. Xu, X. Gu, Z. Cheng, T. Yu, J. Xia, Y. Wei, W. Wu, X. Xie, W. Yin, H. Li, M. Liu, Y. Xiao, H. Gao, L. Guo, J. Xie, G. Wang, R. Jiang, Z. Gao, Q. Jin, J. Wang, B. Cao, Clinical features of patients infected with 2019 novel coronavirus in Wuhan, China. *Lancet* **395**, 497–506 (2020). [doi:10.1016/S0140-6736\(20\)30183-5](https://doi.org/10.1016/S0140-6736(20)30183-5) [Medline](#)
13. W. J. Guan, Z. Y. Ni, Y. Hu, W. H. Liang, C. Q. Ou, J. X. He, L. Liu, H. Shan, C. L. Lei, D. S. C. Hui, B. Du, L. J. Li, G. Zeng, K. Y. Yuen, R. C. Chen, C. L. Tang, T. Wang, P. Y. Chen, J. Xiang, S. Y. Li, J. L. Wang, Z. J. Liang, Y. X. Peng, L. Wei, Y. Liu, Y. H. Hu, P. Peng, J. M. Wang, J. Y. Liu, Z. Chen, G. Li, Z. J. Zheng, S. Q. Qiu, J. Luo, C. J. Ye, S. Y. Zhu, N. S. Zhong; China Medical Treatment Expert Group for Covid-19, Clinical Characteristics of Coronavirus Disease 2019 in China. *N. Engl. J. Med.* (2020). [10.1056/NEJMoa2002032](https://doi.org/10.1056/NEJMoa2002032) [Medline](#)
14. N. Chen, M. Zhou, X. Dong, J. Qu, F. Gong, Y. Han, Y. Qiu, J. Wang, Y. Liu, Y. Wei, J. Xia, T. Yu, X. Zhang, L. Zhang, Epidemiological and clinical characteristics of 99 cases of 2019 novel coronavirus pneumonia in Wuhan, China: A descriptive study. *Lancet* **395**, 507–513 (2020). [doi:10.1016/S0140-6736\(20\)30211-7](https://doi.org/10.1016/S0140-6736(20)30211-7) [Medline](#)
15. J. F. Chan, S. Yuan, K.-H. Kok, K. K.-W. To, H. Chu, J. Yang, F. Xing, J. Liu, C. C.-Y. Yip, R. W.-S. Poon, H.-W. Tsoi, S. K.-F. Lo, K.-H. Chan, V. K.-M. Poon, W.-M. Chan, J. D. Ip, J.-P. Cai, V. C.-C. Cheng, H. Chen, C. K.-M. Hui, K.-Y. Yuen, A familial cluster of pneumonia associated with the 2019 novel coronavirus indicating person-to-person transmission: A study of a family cluster. *Lancet* **395**, 514–523 (2020). [doi:10.1016/S0140-6736\(20\)30154-9](https://doi.org/10.1016/S0140-6736(20)30154-9) [Medline](#)
16. J. F. Chan, K.-H. Kok, Z. Zhu, H. Chu, K. K.-W. To, S. Yuan, K.-Y. Yuen, Genomic characterization of the 2019 novel human-pathogenic coronavirus isolated from a patient with atypical pneumonia after visiting Wuhan. *Emerg. Microbes Infect.* **9**, 221–236 (2020). [doi:10.1080/22221751.2020.1719902](https://doi.org/10.1080/22221751.2020.1719902) [Medline](#)
17. Coronaviridae Study Group of the International Committee on Taxonomy of Viruses, The species Severe acute respiratory syndrome-related coronavirus: Classifying 2019-nCoV and naming it SARS-CoV-2. *Nat. Microbiol.* **5**, 536–544 (2020). [doi:10.1038/s41564-020-0695-z](https://doi.org/10.1038/s41564-020-0695-z) [Medline](#)
18. World Health Organization, www.who.int/docs/default-source/coronaviruse/situation-reports/20200311-sitrep-51-covid-19.pdf?sfvrsn=1ba62e57_4.
19. Supporting information is available on *Science Online*.
20. J. Shi, G. Deng, H. Kong, C. Gu, S. Ma, X. Yin, X. Zeng, P. Cui, Y. Chen, H. Yang, X. Wan, X. Wang, L. Liu, P. Chen, Y. Jiang, J. Liu, Y. Guan, Y. Suzuki, M. Li, Z. Qu, L. Guan, J. Zang, W. Gu, S. Han, Y. Song, Y. Hu, Z. Wang, L. Gu, W. Yang, L. Liang, H. Bao, G. Tian, Y. Li, C. Qiao, L. Jiang, C. Li, Z. Bu, H. Chen, H7N9 virulent mutants detected in chickens in China pose an increased threat to humans. *Cell Res.* **27**, 1409–1421 (2017). [doi:10.1038/cr.2017.129](https://doi.org/10.1038/cr.2017.129) [Medline](#)
21. K. J. Stittelaar, L. de Waal, G. van Amerongen, E. J. Veldhuis Kroeze, P. L. Fraaij, C. A. van Baalen, J. J. van Kampen, E. van der Vries, A. D. Osterhaus, R. L. de Swart,

- Ferrets as a Novel Animal Model for Studying Human Respiratory Syncytial Virus Infections in Immunocompetent and Immunocompromised Hosts. *Viruses* **8**, 168 (2016). [doi:10.3390/v8060168](https://doi.org/10.3390/v8060168) [Medline](#)
22. Q. Zhang, J. Shi, G. Deng, J. Guo, X. Zeng, X. He, H. Kong, C. Gu, X. Li, J. Liu, G. Wang, Y. Chen, L. Liu, L. Liang, Y. Li, J. Fan, J. Wang, W. Li, L. Guan, Q. Li, H. Yang, P. Chen, L. Jiang, Y. Guan, X. Xin, Y. Jiang, G. Tian, X. Wang, C. Qiao, C. Li, Z. Bu, H. Chen, H7N9 influenza viruses are transmissible in ferrets by respiratory droplet. *Science* **341**, 410–414 (2013). [doi:10.1126/science.1240532](https://doi.org/10.1126/science.1240532) [Medline](#)
 23. M. Imai, T. Watanabe, M. Hatta, S. C. Das, M. Ozawa, K. Shinya, G. Zhong, A. Hanson, H. Katsura, S. Watanabe, C. Li, E. Kawakami, S. Yamada, M. Kiso, Y. Suzuki, E. A. Maher, G. Neumann, Y. Kawaoka, Experimental adaptation of an influenza H5 HA confers respiratory droplet transmission to a reassortant H5 HA/H1N1 virus in ferrets. *Nature* **486**, 420–428 (2012). [doi:10.1038/nature10831](https://doi.org/10.1038/nature10831) [Medline](#)
 24. S. Herfst, E. J. A. Schrauwen, M. Linster, S. Chutinimitkul, E. de Wit, V. J. Munster, E. M. Sorrell, T. M. Bestebroer, D. F. Burke, D. J. Smith, G. F. Rimmelzwaan, A. D. M. E. Osterhaus, R. A. M. Fouchier, Airborne transmission of influenza A/H5N1 virus between ferrets. *Science* **336**, 1534–1541 (2012). [doi:10.1126/science.1213362](https://doi.org/10.1126/science.1213362) [Medline](#)
 25. J. M. van den Brand, B. L. Haagmans, L. Leijten, D. van Riel, B. E. E. Martina, A. D. M. E. Osterhaus, T. Kuiken, Pathology of experimental SARS coronavirus infection in cats and ferrets. *Vet. Pathol.* **45**, 551–562 (2008). [doi:10.1354/vp.45-4-551](https://doi.org/10.1354/vp.45-4-551) [Medline](#)
 26. B. E. Martina, B. L. Haagmans, T. Kuiken, R. A. M. Fouchier, G. F. Rimmelzwaan, G. Van Amerongen, J. S. M. Peiris, W. Lim, A. D. M. E. Osterhaus, Virology: SARS virus infection of cats and ferrets. *Nature* **425**, 915 (2003). [doi:10.1038/425915a](https://doi.org/10.1038/425915a) [Medline](#)
 27. Y. K. Chu, G. D. Ali, F. Jia, Q. Li, D. Kelvin, R. C. Couch, K. S. Harrod, J. A. Hutt, C. Cameron, S. R. Weiss, C. B. Jonsson, The SARS-CoV ferret model in an infection-challenge study. *Virology* **374**, 151–163 (2008). [doi:10.1016/j.virol.2007.12.032](https://doi.org/10.1016/j.virol.2007.12.032) [Medline](#)
 28. Novel Coronavirus Pneumonia Emergency Response Epidemiology Team, The epidemiological characteristics of an outbreak of 2019 novel coronavirus diseases (COVID-19) in China. [in Chinese] *Zhonghua Liu Xing Bing Xue Za Zhi* **41**, 145–151 (2020). [doi:10.3760/cma.j.issn.0254-6450.2020.02.003](https://doi.org/10.3760/cma.j.issn.0254-6450.2020.02.003) [Medline](#)
 29. R. Yan, Y. Zhang, Y. Li, L. Xia, Y. Guo, Q. Zhou, Structural basis for the recognition of SARS-CoV-2 by full-length human ACE2. *Science* **367**, 1444–1448 (2020). [doi:10.1126/science.abb2762](https://doi.org/10.1126/science.abb2762) [Medline](#)
 30. M. Letko, A. Marzi, V. Munster, Functional assessment of cell entry and receptor usage for SARS-CoV-2 and other lineage B betacoronaviruses. *Nat. Microbiol.* **5**, 562–569 (2020). [doi:10.1038/s41564-020-0688-y](https://doi.org/10.1038/s41564-020-0688-y) [Medline](#)
 31. The *Cell* Editorial Team, Embracing the Landscape of Therapeutics. *Cell* **181**, 1–3 (2020). [doi:10.1016/j.cell.2020.03.025](https://doi.org/10.1016/j.cell.2020.03.025) [Medline](#)
 32. Q. Zhang *et al.*, bioRxiv (2020). <https://doi.org/10.1101/2020.04.01.021196>.
 33. H. Yang, Y. Chen, C. Qiao, X. He, H. Zhou, Y. Sun, H. Yin, S. Meng, L. Liu, Q. Zhang, H. Kong, C. Gu, C. Li, Z. Bu, Y. Kawaoka, H. Chen, Prevalence, genetics, and

- transmissibility in ferrets of Eurasian avian-like H1N1 swine influenza viruses. *Proc. Natl. Acad. Sci. U.S.A.* **113**, 392–397 (2016). [doi:10.1073/pnas.1522643113](https://doi.org/10.1073/pnas.1522643113) [Medline](#)
34. X. Li, J. Shi, J. Guo, G. Deng, Q. Zhang, J. Wang, X. He, K. Wang, J. Chen, Y. Li, J. Fan, H. Kong, C. Gu, Y. Guan, Y. Suzuki, Y. Kawaoka, L. Liu, Y. Jiang, G. Tian, Y. Li, Z. Bu, H. Chen, Genetics, receptor binding property, and transmissibility in mammals of naturally isolated H9N2 Avian Influenza viruses. *PLOS Pathog.* **10**, e1004508 (2014). [doi:10.1371/journal.ppat.1004508](https://doi.org/10.1371/journal.ppat.1004508) [Medline](#)
35. D. van Riel, V. J. Munster, E. de Wit, G. F. Rimmelzwaan, R. A. M. Fouchier, A. D. M. E. Osterhaus, T. Kuiken, H5N1 Virus Attachment to Lower Respiratory Tract. *Science* **312**, 399 (2006). [doi:10.1126/science.1125548](https://doi.org/10.1126/science.1125548) [Medline](#)